



Title	Simultaneous effects of airflow and temperature increase on water removal in bio-drying
Author(s)	Ham, Geun-Yong; Lee, Dong-Hoon; Matsuto, Toshihiko; Tojo, Yasumasa; Park, Jae-Ram
Citation	Journal of material cycles and waste management, 22(4), 1056-1066 <a href="https://doi.org/10.1007/s10163-020-01000-x">https://doi.org/10.1007/s10163-020-01000-x</a>
Issue Date	2020-07
Doc URL	<a href="http://hdl.handle.net/2115/82105">http://hdl.handle.net/2115/82105</a>
Rights	This is a post-peer-review, pre-copyedit version of an article published in Journal of material cycles and waste management. The final authenticated version is available online at: <a href="http://dx.doi.org/10.1007/s10163-020-01000-x">http://dx.doi.org/10.1007/s10163-020-01000-x</a> .
Type	article (author version)
File Information	Manuscript_HAM_revised.pdf



[Instructions for use](#)

1 **Original article**

2 **Simultaneous Effects of Airflow and Temperature Increase on Water removal in Bio-**  
3 **drying**

4 Geun-Yong Ham<sup>1</sup>, Dong-Hoon Lee<sup>2</sup>, Toshihiko Matsuto<sup>1\*</sup>, Yasumasa Tojo<sup>1</sup>, Jae-Ram Park<sup>2</sup>

5 <sup>1</sup> Laboratory of Solid Waste Disposal Engineering, Faculty of Engineering, Hokkaido  
6 University, Kita 13, Nishi 8, Kita-ku, Sapporo, Hokkaido 060-8628, Japan

7 <sup>2</sup> Department of Environmental Engineering, University of Seoul, 163 Seoulsiripdaero,  
8 Dongdaemun-gu, Seoul 02504, Republic of Korea

9

10 Geun-Yong Ham: [gyham127@gmail.com](mailto:gyham127@gmail.com)

11 Dong-Hoon Lee: [dhlee@uos.ac.kr](mailto:dhlee@uos.ac.kr)

12 Yasumasa Tojo: [tojo@eng.hokudai.ac.jp](mailto:tojo@eng.hokudai.ac.jp)

13 Jae-Ram Park: [fuel3079@nate.com](mailto:fuel3079@nate.com)

14

15 \* Corresponding author. Tel./fax: +81 11 706 6825

16 E-mail address: [matsuto@eng.hokudai.ac.jp](mailto:matsuto@eng.hokudai.ac.jp)

17

18 **ABSTRACT**

19 Bio-drying MBT is a type of mechanical biological treatment (MBT) system, whereby  
20 the aerobic biological process is first used to remove moisture, which is followed by the  
21 mechanical separation to recover material and energy as a solid recovered fuel (SRF). Among  
22 various parameters of this process, the simultaneous effects of airflow rate and organic  
23 contents were examined in this study. A 25 L acrylic column reactor was filled with  
24 simulated waste. Temperature and humidity of the air inlet and outlet were continuously  
25 monitored, and CO<sub>2</sub> concentrations in outlet air were periodically analyzed to observe aerobic  
26 biodegradation as well as metabolic water generation. Based on the data, the different water  
27 removal contributions by airflow and biodegradation were compared and finally evaluation of

28 the inter-dependence of parameters and feedback effect in the bio-drying process was carried  
29 out. While the biodegradation of organics induced a significant amount of water removal due  
30 to increased temperature, high organic content has a negative effect on water removal by  
31 generating metabolic water. Water removal by air replacement is greater than that associated  
32 with temperature increases caused by biodegradation. However, excessive airflow rate can  
33 terminate biodegradation by drastically lowered moisture content even though organics  
34 remained.

35

36 Keywords: Bio-drying, Organic content, Airflow rate, Water removal rate

37

38

## 39 **Introduction**

40 Historically, most EU countries disposed of substantially mixed municipal solid waste  
41 (MSW) in landfills without any type of pretreatment. High proportions of biodegradable  
42 wastes have been discarded in landfills, which resulted in a need for long-term care to  
43 manage the leachate and landfill gas emission caused from the biodegradation of organic  
44 matter in the waste [1]. To deal with this issue, in the late 1990s, the European Commission  
45 established the Landfill Directive (99/31/EC) [2], which required the diversion of  
46 biodegradable waste from landfills. In response to this directive, mechanical biological  
47 treatment (MBT) systems have emerged to reduce the amount of biodegradable waste sent to  
48 the landfill. A typical MBT system begins with mechanical separation of mixed MSW, which  
49 is then followed by biological treatment to remove the organics and thermal treatment for the  
50 remaining combustible fraction. The biologically and/or thermally stabilized residue from  
51 these processes is sent to a landfill for disposal. Biogas is recovered when the organic fraction  
52 is treated by anaerobic digestion, and energy is recovered as a solid fuel or through thermal  
53 treatment, and dry recyclables are also recovered [3].

54 Bio-drying MBT is a type of MBT system, in which an aerobic biological process is  
55 first used to remove moisture, followed by mechanical separation to recover material and  
56 energy as a solid recovered fuel (SRF). SRFs can be burned in cement kilns or other co-  
57 combustion power plants as a fuel, which conserves the conventional energy sources  
58 typically used for those kinds of operations [4, 5].

59 In a previous study on bio-drying, the effects of several parameters were examined,  
60 including aeration (airflow rate (AFR), frequency), waste properties (waste type, moisture  
61 content, organic content (OC)), and bulking agents (type, mixing ratio) used to adjust the  
62 OCs or moisture contents. Among them, the AFR and OC have been considered as the  
63 primary parameters, and these two parameters were investigated in this study. The

64 simultaneous effects of the AFR and OC were also studied by Huiliñir and Villegas and  
65 Colomer-Mendoza et al. [6, 7]. Huiliñir and Villegas used sludge from a wastewater  
66 treatment plant used for the slaughterhouse and investigated the AFR (1, 2, and 3 L/min·kg-  
67 TS) and OC by changing the ratio of the bulking agents (10%, 23%, and 33%), which  
68 resulted in different initial moisture content values of 59%, 68%, and 78%, respectively.  
69 Colomer-Mendoza et al. studied AFR (0.88 to 6.42 L/min·kg-TS) and the bulking agent ratio  
70 (0% and 15% of mixture) in the bio-drying of garden waste.

71 Other studies have investigated AFR, OC, and other parameters. Adani et al. studied  
72 AFR (0.1–0.4 L/min·kg-TS) in bio-drying of MSW [8], and Navaee-Ardeh et al. investigated  
73 AFR (25–75 m<sup>3</sup>/h) in a bio-drying process that utilized paper and pulp mill sludge as the  
74 feedstock [9]. While other studies have been conducted as batch processes, bio-dried sludge  
75 was recirculated in a study by Navaee-Ardeh et al. [9]. The effect of OCs was investigated by  
76 Yang et al. using different concentration of glucose and ground food waste that were mixed  
77 with bio-dried sludge for inoculation [10]. In addition to the AFR and bulking agent ratio, the  
78 type of bulking agent, such as sawdust, wood pellets, straw, and corncob [11–13] and initial  
79 moisture content for sewage sludge bio-drying [11], and inoculation ratio [13] have also been  
80 studied.

81 In the bio-drying process, moisture is removed by the combined actions of aeration  
82 and biodegradation. Generated metabolic heat increases the temperature inside the reactor,  
83 and this facilitates the moisture evaporation from the waste. Air then carries the evaporated  
84 vapor and discharges it to the atmosphere. Measuring the weight of the waste before and after  
85 the experiment is the most common method of determining changes in moisture content.  
86 However, this only shows the change in the water amount. To estimate certain ongoing  
87 phenomena during the process, temperature, relative humidity in the airflow, and CO<sub>2</sub>  
88 concentrations must be continuously measured, and metabolic water generation should be  
89 taken into account. Among the previous studies, such continuous monitoring was performed

90 by Cai et al., Huiliñir and Villegas and Navaee-Ardeh et al. [6, 9, 14]. However, Cai et al. and  
91 Huiliñir and Villegas estimated the metabolic water generation through the measurement of  
92 VS changes by periodic waste sampling, whereas Navaee-Ardeh et al. estimated metabolic  
93 water generation by changes in the CO<sub>2</sub> concentration, but only the AFR was changed as an  
94 experimental condition.

95 Compared with the previously conducted studies that we reviewed, the novelty of our  
96 approach is characterized by the monitoring of the simultaneous effects of OC and AFR to  
97 balance moisture, including metabolic water generation determined by continuous  
98 measurement of the airflow. To establish the moisture balance, inlet and outlet flow of  
99 moisture were estimated by continuous measurement of temperature and relative humidity of  
100 the air. CO<sub>2</sub> concentrations in the outlet air were periodically analyzed to observe aerobic  
101 biodegradation as well as metabolic water generation. Furthermore, contributions from the  
102 AFR and temperature increase on water removal were quantitatively compared.

103

## 104 **Materials and methods**

### 105 **Experimental equipment**

106

107 **Fig. 1** Schematic view of the reactor used in the bio-drying experiment

108

109 As shown in Fig. 1, the reactor used in this study was a 25 L acrylic cylindrical  
110 reactor with a diameter of 20 cm and a height of 70 cm. The reactor was filled with simulated  
111 wastes on a perforated base plate to ensure uniform air distribution from 30 to 60 cm in the  
112 reactor. The upper portion was covered with an acrylic lid with a hole for air exhaust. The  
113 reactor was insulated with a 5 cm thick layer of Styrofoam. A blower was connected to the

114 bottom of the reactor with Teflon tubing. Ambient air was introduced via the blower and  
115 moved upward through the reactor toward the exhaust port in the lid. Heat loss through  
116 reactor wall by conduction and radiation is negligible because the loss is less than 1 % of  
117 energy consumption for evaporation and temperature increase of air and solid materials in  
118 lab-scale bio-drying reactor insulated with 100-mm of a hollow cotton wall [15].

119 The experiments were conducted from March to May 2015 and July to August 2016. All the  
120 experiments were conducted in a temperature-controlled room at  $30\text{ }^{\circ}\text{C} \pm 1\text{ }^{\circ}\text{C}$ . The reactor  
121 was placed on an electronic scale (FG-60KBM-H, AND, Korea), and the total weight was  
122 measured and manually recorded at 12 h intervals. Each experimental run was terminated  
123 when the temperature of outlet air reached that of the ambient air.

#### 124 **Measurement and analysis**

125 The temperature and humidity of the inlet and outlet air were monitored by a  
126 humidity-temperature meter (TES-1365, TES, Taiwan). Three temperature sensors were  
127 installed (two inside the reactor and the one at the outlet port in the lid) and connected to a  
128 thermometer (TES-1384, TES, Taiwan). The data logging interval was set to 4 min for  
129 monitoring both ports. Inlet and outlet gas were sampled every 12 h to quantify  $\text{CO}_2$   
130 concentrations by gas chromatography (GC-2014, Shimadzu, Japan). An in-line gas flow  
131 meter (RMA, Dwyer, United States) was used to monitor the AFR.

132 At the end of all experimental runs, simulated waste was taken from the reactor, and  
133 the final weight was measured. After weighing, the moisture content of the product was  
134 determined by oven drying (forced convection drying oven, Chang Shin scientific co., Korea)  
135 at  $80\text{ }^{\circ}\text{C}$ .

#### 136 **Experimental condition**

137 In the experiment, commercial dog food (Prime Balance, Nutrena, Korea) was used to  
138 represent easily biodegradable matter in the simulated waste. Nakasaki et al. and Chang et al.  
139 reported that dry dog food can represent the easily biodegradable organic matter, and they  
140 demonstrated good reproducibility, which resulted in uniform properties at the beginning and  
141 end of the experiment [16, 17]. According to the nutrition level in the dog food used in this  
142 experiment, it consisted primarily of carbohydrates (70% d.w.), crude protein (14% d.w.),  
143 crude fat, crude fiber, and miscellaneous elements. Based on elemental compositions (C  
144 44.7%, H 6.3%, N 2.4%, O 39.0%, ash 7.6% dry basis) determined by the authors, the  
145 chemical composition of the VS was estimated to be  $C_{21}H_{36}O_{14}N$ .

146 OC was controlled by changing the ratio of dog food to wood pellets and included  
147 10%, 25%, 50%, 75%, and 100%, by mass. Although the dog food is not 100%  
148 biodegradable, its dry basis ratio is referred to as OC for the purpose of this study. The wood  
149 pellets were assumed to be non-degradable during the bio-drying process due to their  
150 relatively low biodegradability in the relatively short process time of the experiment [12]. As  
151 a simulated waste, 3.1 kg of the dog food and wood pellet mixture with the previously  
152 mentioned ratios was placed in the column reactor, and the initial moisture content was set at  
153 40% by adding distilled water. Forty percent of the initial moisture content was determined  
154 after measuring the field capacity of the dog food. With over 50% of moisture content, the  
155 dog food easily becomes broken down. Return activated sludge, which was collected from a  
156 commercial wastewater treatment facility, was injected to inoculate the simulated waste and  
157 was equal to 10% of the dog food mass on a dry basis.

158 Regarding aeration, it has been suggested that the recommended aeration rates depend  
159 on the substrate in the composting process [18]. The bio-drying process is a modified  
160 composting process but focused more on water removal. Therefore, a slightly higher range of  
161 AFR can be applied. In this study, the operation range applied in the past study, 0.4–1.1  
162 L/min·kgVS, was used by referring to Adani et al. and Colomer-Mendoza et al. [7, 8]. When



163 the initial OC was 100%, 0.4 L/min·kgVS was multiplied by 3.1 kg, resulting in a value of  
164 1.2, which corresponded to approximately 1 L/min. Therefore, the AFRs selected for  
165 experimental analysis were set at 1, 2, and 3 L/min.

166

167 **Table 1.** Different variables and initial conditions in the experiments

168 Table 1 summarizes the experimental conditions employed in this study. All the  
169 experimental runs were identified by the initial OC and AFR, such as “10-1” (i.e., 10% OC  
170 and a flowrate of 1 L/min). The average relative humidity (RH) of the inlet air in each  
171 experiment depended on the season. Table 1 presents the total days of operation, initial  
172 organic matter (dog food), and final organic matter and moisture content. The equations  
173 presented in next section were used to estimate final values.

174

## 175 **Model**

### 176 **Model equations**

177 The moisture balance in the reactor can be described by Eqs. (1) and (2).

$$178 \quad \Delta w_{\text{nom}} \text{ (kg/h)} = (V_{\text{out}} \times X_{\text{out}} \times 10^{-3}) - (V_{\text{in}} \times X_{\text{in}} \times 10^{-3}) \quad (1)$$

$$179 \quad \Delta w_{\text{act}} \text{ (kg/h)} = \Delta w_{\text{nom}} - \Delta w_{\text{gen}} \quad (2)$$

180 where V is AFR in m<sup>3</sup>/h, and X represents the water vapor content per unit volume of air, in  
181 g/m<sup>3</sup>. Eq. (1) is the water removal rate determined by the difference between moisture  
182 measured at the inlet and outlet of the airflow on a per hour basis, but it was nominal without  
183 considering the metabolic water generation ( $\Delta w_{\text{gen}}$ ). Therefore, the actual water removal rate,  
184  $\Delta w_{\text{act}}$ , was calculated using Eq. (2).

185

186 **Table 2.** Equations used for mass and heat balance

187

188 Table 2 summarizes other equations used in the model, and the nomenclature is  
189 provided at the end of this paper. The outlet AFR ( $V_{out}$ ) was calculated by considering the  
190 change in air density of the inlet airflow ( $V_{in}$ ) (Eq. (3)). X, which denotes the water vapor  
191 content per volume of air, was calculated using Eq. (4) as a function of water vapor pressure  
192 (pv). The maximum value of water vapor pressure that can be reached at any temperature is  
193 defined as the saturated water vapor pressure (pvs). The ratio between pv and pvs is the RH.

194 For biodegradation, it was assumed that the organics were fully degraded which can  
195 thus be expressed by Eq. (7). CO<sub>2</sub> generation rate ( $\Delta C_{gen}$ ) was estimated by the difference  
196 between the CO<sub>2</sub> concentrations in the air at the inlet and outlet (Eq. (8)). Degraded organics  
197 and generated metabolic water per unit time can be calculated using Eqs. (9) and (10), which  
198 are based on Eq. (8).

199 The mass of organics ( $M_o$ ) and moisture (W) at a particular time or its change during  
200 a particular period of time can be estimated by the integration of each rate ( $\Delta M_o$ ,  $\Delta w$ ).  
201 Moisture content (MC) can be calculated by the ratio between water mass to total waste mass  
202 at a specific time, and OC was estimated by the ratio of  $M_o$  to total dry mass.

203 The rate of heat generation,  $\Delta Q_{gen}$ , was calculated using Eq. (11) by multiplying the  
204 reaction heat of the degraded organics. Spoehr and Milner suggested the empirical method for  
205 calculating the heat of combustion for any type of organic matter is expressed by Eq. (12),

$$206 \quad Q \text{ (kJ/kg)} = \left( 127 \times \frac{\{100 \times (2.66 \times C\% + 7.94 \times H\% - O\%)\}}{398.9} + 400 \right) \times \frac{4.184 \text{ kJ}}{1 \text{ kcal}} \quad (12)$$

207 where Q is the heat of combustion for degraded organics, and C%, H%, and O% are the  
208 weight percentages of carbon, hydrogen, and oxygen, respectively, on an ash-free basis [19].

209 For the dog food used in this study, its heat of combustion was estimated to be 20406 kJ/kg.

210 Heat transfer in the inlet and outlet airflow ( $\Delta Q_{in}$  and  $\Delta Q_{out}$ ) is calculated using the sum of  
211 dry air and water vapor enthalpy by applying Eq. (13).

## 212 **Example of model output**

213 **Fig. 2** Experimental data and model output of run “50-3” (a) Temperature and CO<sub>2</sub>  
214 concentration profiles (Measured), (b) Rate of water mass changes in balance (Estimated), (c)  
215 Heat profiles (Estimated)

216

217 As an example of model output, Fig. 2 shows the time profile for the run 50-3 (i.e., 50%  
218 of initial OC and a 3 L/min inlet AFR). The average inlet RH was 14.0% (see Table 1).  
219 Values in Fig. 2a were measured, and the others were calculated using the model in Table 2.  
220 During the initial period when biodegradation had not yet begun, which is referred to as “w/o  
221 BIO” in the figure,  $T_{in}$  and  $T_{out}$  were held constant, and the slight decrease of  $T_s$  was due to  
222 heat loss associated with evaporation.

223 After one day, CO<sub>2</sub> concentrations began to increase, which is indicative of a  
224 biodegradation process at work. The integrated area under the CO<sub>2</sub> curve presents the extent  
225 of organic degradation. During the biodegradation period, referred to as “w/ BIO,” nominal  
226 water removal rate ( $\Delta W_{nom}$ ) increased as  $T_{out}$  increased. This is one of the fundamental  
227 features of bio-drying, though actual water removal rate ( $\Delta W_{act}$ ) was decreased by metabolic  
228 water generation rate ( $\Delta W_{gen}$ ).

229 Microbial biodegradation of organic matter gradually decreased after it peaked at its  
230 maximum. Either remaining OC or MC could have affected microbial activity, which is  
231 discussed in detail later. Fig. 2c shows the heat balance. The difference between  $\Delta Q_{gen}$  and  
232  $\Delta Q_{out}$  was indicative of the heat used for evaporation or loss from the reactor.

## 233 **Reliability of model**

234

235 **Fig. 3** Comparison of actual removed water mass ( $W_{act}$ ) between experiment and model  
236 during entire experimental period

237

238 The mass of removed water ( $W_{act}$ ) calculated by the model (integration of  $\Delta w_{act}$ ) was  
239 compared with that of the experiments during entire experimental period, as shown in Fig. 3,  
240 where each label indicates the initial OC. The magnitude of error is generally within 20%.  
241 Therefore, the model estimated the bio-drying phenomena reasonably well.

242

## 243 **Discussion**

### 244 **Drying mechanism in the bio-drying process**

245

246 **Fig. 4** Temperature dependence of  $p_{vs}$  and  $X_{sat}$  and increase of water vapor pressure ( $p_v$ ) in  
247 bio-drying process

248

249 Drying is a process of moisture transfer from the surface of waste to air. Evaporation  
250 is driven by the differences of water vapor pressure between the surface of the waste and air.  
251 The required heat for evaporation is obtained from the surroundings. Since the RH of the  
252 outlet air was always 100% in all experimental runs,  $p_v$  at inlet temperature increase to  $p_{vs}$  at  
253 outlet temperature. The driving force of evaporation can be expressed as the gap between two  
254 points, i.e., outlet on the  $p_{vs}$  curve and inlet in Fig. 4. As the temperature increased, the  $p_{vs}$   
255 in the air increased so as  $X_{sat}$ .

256

257 The change of  $p_v$  (water vapor pressure) in the air from the inlet to outlet is  
258 schematically shown by the broken arrow in Fig. 4. In w/o BIO period, before biological  
decomposition occurred, there were no increases in temperature due to the absence of heat

259 associated with biodegradation. Consequently, the water vapor pressure  $p_v$  in the air  
260 increased only up to the  $p_{vs}$  (saturated water vapor pressure) at the same temperature when it  
261 was introduced into the reactor. However, once biodegradation proceeded under w/ BIO  
262 period, the heat generation increased the waste temperature. Simultaneously, the initial  
263 driving force of evaporation increased dramatically due to a high  $p_{vs}$ , which was indicative  
264 of an increase in the water content in the outlet air,  $X_{out}$ .

265 Water removal rate is increased with biodegradation as shown in Fig. 4, and the  
266 airflow carried saturated vapor out of the reactor. In w/o BIO period, only the influence of  
267 AFR can be discussed, and the relationship  $1 - (RH/100) = (\Delta W_{act} = \Delta W_{nom})$  in this case) for  
268 different AFR by taking  $1 - (RH/100)$  as x-axis (Fig. 5). The higher the AFR, the more water  
269 was removed, and simultaneously, the lower the RH of the inlet air, which resulted from the  
270 large amount of water removal associated with the increasing gap between the  $p_{vs}$  and the  $p_v$ .

271

272 **Fig. 5** Relations between water removal rate and RH of inlet air under different AFR during  
273 w/o BIO period

274

275 In Fig. 5, a regression line for AFR = 1 L/min was first determined by assuming the  
276 removal rate was zero at an RH of inlet air = 100%, whereby the lines for AFR = 2 L/min and  
277 3 L/min are simply multiplied by 2 and 3, respectively. That is, AFR has simply the  
278 replacement effect of saturated air in the reactor.

279 **Biodegradation of organic matter and its limitation**

280

281 **Fig. 6** CO<sub>2</sub> generation rate and moisture content profiles during entire experimental period (a)  
282 AFR 1 L/min, (b) AFR 3 L/min

283

284 Different initial conditions of the OC and AFR induced different biodegradation  
285 characteristics. To observe the extent of biodegradation, the CO<sub>2</sub> generation rate ( $\Delta C_{\text{gen}}$ ) and  
286 MC profiles are shown in Fig. 6. The  $\Delta C_{\text{gen}}$ , expressed in kmol/h, is calculated using the  
287 AFR and CO<sub>2</sub> concentrations in the outlet air (Eq. (8)). The integration of each curve is  
288 proportional to the amount of degraded OC. The numbers in parenthesis indicate the initial  
289 and final OC, which are defined by the ratio of organics to total dry solids.

290 CO<sub>2</sub> generation rate curves of all runs were bell-shaped and had longer tails at lower  
291 AFRs and higher OC values. In runs with the AFR set at 3 L/min (Fig. 6b), biodegradation  
292 did not continue very long compared to the runs with lower AFRs because microbial activity  
293 was limited by low levels of MC, even though sufficient OC was still available (i.e., 19%,  
294 42%, and 83% corresponding to initial OC values of 25%, 50%, and 100%, respectively).  
295 The low MC was caused by high AFR values that rapidly carried out all vaporized water.

296 By contrast, in runs using an AFR of 1 L/min, biodegradation continued for a longer  
297 period of time until the OC decreased to 12% and 27%, corresponding to initial OC values of  
298 25% and 50%, respectively. During the experiment, MC was maintained around 40% due to  
299 the low AFR. In this case, biodegradation was terminated due to the low concentrations of  
300 organics, not by moisture. In run 100-1, biological degradation ceased in spite of 67% of the  
301 organics remaining because the feed material was composed only of dog food. Without  
302 bulking material (i.e., wood pellets), the dog food stuck together, and the biodegradation was  
303 limited due to a reduction in the contact area associated with short-circuiting of the airflow  
304 around larger masses of dog food.

### 305 **Effects of air flow and biodegradation**

306

307 **Fig. 7** Conceptual diagram of water removal rate in the bio-drying process

308

309 Fig. 7 depicts a conceptual diagram of the water removal rate in the bio-drying  
310 process. Metabolic water generation rate ( $\Delta w_{gen}$ ) is depicted as a negative value to indicate  
311 added water by bio-drying process, and the water removal rate during the w/o BIO period is  
312 denoted as  $\Delta w_{air}$ . From this figure, the following three water removal rates during the w/ BIO  
313 period can be defined.

314 Effect of airflow:  $\Delta w_{air}$

315 Effect of temperature increase (nominal):  $\Delta w_{nom} - \Delta w_{air}$

316 Effect of temperature increase (actual):  $\Delta w_{nom} - \Delta w_{air} - \Delta w_{gen}$

317 Given that the time profile was different among experiments (refer to Fig. 6), a  
318 comparison of the water removal rate and maximum temperature of the simulated waste at  
319 the peak point of CO<sub>2</sub> concentration for all the runs is shown in Fig. 8.

320

321 **Fig. 8** Water removal rate defined in Fig. 7 at the peak point of CO<sub>2</sub> concentration (a) AFR 1  
322 L/min, (b) AFR 3 L/min

323

324 Except for the runs with 10% of the initial amount of OC, where less heat generation  
325 occurred due to the small amount of organic matter, the maximum temperature of the outlet  
326 air ranged between 45 °C and 50 °C. The metabolic water generation rate,  $\Delta w_{gen}$ , remained  
327 virtually constant regardless of AFR and initial OC. A constant  $\Delta w_{gen}$  indicates that  
328 biodegradation rate at peak time did not depend on the experimental conditions in this study.

329 Compared with the Fig. 8a and Fig. 8b, the nominal effect of temperature increase  
330 ( $\Delta w_{nom} - \Delta w_{air}$ ) on water removal remarkably increased as the AFR increased, but so did  
331  $\Delta w_{air}$ . Airflow replace the saturated vapor as mentioned in previous section, so replaced  
332 volume of air is proportionately increased with AFR in unit time. To exclude the increased

333 effect of replaced air, each water removal rate was divided by the AFR,  $(\Delta W_{\text{nom}} - \Delta W_{\text{air}}) / V$   
334 and  $\Delta W_{\text{air}} / V$ , as shown by the broken line in Fig. 8b, and these were similar to the result  
335 when the AFR was 1 L/min. Therefore, the effect of airflow was higher than the temperature  
336 increase.

337 As a result, the actual water removal rate, which was determined by the difference  
338 between  $(\Delta W_{\text{nom}} - \Delta W_{\text{air}})$  and  $\Delta W_{\text{gen}}$  curves also increased with AFR because  $\Delta W_{\text{gen}}$  remained  
339 virtually constant regardless of the AFR.

#### 340 **Total water removal during w/ BIO period**

341 The previous section discussed the water removal rate at the peak point of  $\text{CO}_2$   
342 concentration. However, the efficiency of drying should be evaluated by the total amount of  
343 removed water throughout the experiment period. In Fig. 9, the integrated amount of water  
344 removal during the w/ BIO period is shown.

345

346 **Fig. 9** Removed water mass during w/ BIO period (a) Comparison of nominal removed water  
347 mass ( $W_{\text{nom}}$ ) and actual removed water mass ( $W_{\text{act}}$ ), (b) Effect of temperature increase  
348 ( $W_{\text{nom}} - W_{\text{air}}$ ,  $W_{\text{nom}} - W_{\text{air}} - W_{\text{gen}}$ ) on water removal compared with the effect of airflow ( $W_{\text{air}}$ )

349

350 As shown in Fig. 9a, the amount of nominal removed water mass,  $W_{\text{nom}}$ , increased as  
351 the initial OC increased. This was caused by the difference in the duration of aerobic  
352 biodegradation. In other words, as shown in Fig. 6a, when the initial OC is high, the aerobic  
353 reaction continued for a longer period of time. Therefore, the amount of moisture removal  
354 increased with a higher water vapor pressure (pvs) and with a longer duration of saturated  
355 vapor replaced by airflow.

356 There was little difference by AFR in  $W_{\text{nom}}$  (Fig. 9a), because the shorter duration of  
357 the aerobic reaction associated with high AFR was made up or vice versa (see Fig. 6). The



358 duration of active biodegradation is shown in Fig. 9a. On the other hand,  $W_{act}$  significantly  
359 decreased in lower AFR runs because of the considerable amount of metabolic water  
360 generation by long biodegradation. Meanwhile, aerobic biodegradation was terminated due to  
361 low MC (see Fig. 6b) which resulted from the significant replacement of moisture by a high  
362 AFR.

363 Finally, the effect of temperature increase compared with the effect of AFR on water  
364 removal is presented in Fig. 9b.  $(W_{nom}-W_{air})$  refers to the water mass removed by increases in  
365 temperature and  $(W_{nom}-W_{air}-W_{gen})$  shows the ultimate amount of water removed, including  
366 the negative effect of added metabolic water. All points were plotted against  $W_{air}$ , which is  
367 the water removal solely associated with aeration. OC values of 10%, 50%, and 100% are  
368 plotted for comparison among all runs, and each OC is represented with different marks.

369 In each AFR condition, the higher the initial OC, both  $W_{air}$  and  $(W_{nom}-W_{air})$  increased  
370 due to the longer period of elapsed time, which maximizes the effect of increases in  
371 temperature. However, when metabolic water is taken into account, the actual water removal  
372  $(W_{nom}-W_{air}-W_{gen})$  by biodegradation decreased at lower AFR values, which was especially  
373 true in runs 10-1 and 50-1 that showed negative values or values close to zero due to the  
374 reduced replacement effect. In case 100-1, agglomerated feed materials interrupted the air  
375 passage, and this resulted in less biodegradation as well as less metabolic water generation.  
376 When comparing the x- and y-axis values of  $(W_{nom}-W_{air}-W_{gen})$ , which are equal to the actual  
377 water removal, the effects of temperature increase associated with biodegradation on water  
378 removal were always lower than those associated with air replacement.

379

## 380 **Conclusion**

381

382 **Fig. 10** Overall water removal mechanism in the bio-drying process

383

384            Fig. 10 summarizes the overall water removal mechanism in the bio-drying process  
385 under different initial conditions, including variations in OC (organic content), AFR (airflow  
386 rate), and RH (relative humidity) of the inlet air. Evaporation is driven by the difference  
387 between the  $p_{vs}$  (saturated water vapor pressure) of the waste surface and the  $p_v$  (water vapor  
388 pressure) in the passing air, and this driving force increased either due to temperature  
389 increases associated with biodegradation or the dryness of introducing air. However, high OC  
390 was a negative contribution with respect to water removal due to the generation of metabolic  
391 water. On the other hand, saturated vapor in the reactor was carried out by airflow, so high  
392 AFR enhanced the water removal rate. Water removal associated with air replacement was  
393 generally greater than that associated with temperature increases caused by biodegradation.  
394 But excessive AFR would terminate biodegradation due to the reduction in MC even though  
395 organics remained.

396            In the bio-drying process, all the parameters are interdependent, and there are several  
397 feedback loops as previously mentioned. The findings of this study can be used for the design  
398 and operation of a full-scale system.

399

## Appendix

Nomenclature			
Symbol		Unit	Definition
State variables	t	days	Time
	T	°C	Temperature
	V	m <sup>3</sup> /h	Airflow rate
	CO <sub>2</sub>	%	CO <sub>2</sub> concentration
	X	g/m <sup>3</sup>	Water vapor per unit air volume
	RH	%	Relative humidity
	ρ <sub>a</sub>	kg/m <sup>3</sup>	Density of dry air
	p <sub>v</sub>	Pa	Water vapor pressure
	p <sub>vs</sub>	Pa	Saturated water vapor pressure
Decomposition	M <sub>o</sub>	kg	Organic mass
	ΔM <sub>o</sub>	kg/h	Organic degradation rate
	ΔC <sub>gen</sub>	kmol/h	CO <sub>2</sub> generation rate
	OC	%	Organic content
Moisture	W	kg	Water mass
	Δw	kg/h	Water removal rate
	Δw <sub>gen</sub>	kg/h	Metabolic water generation rate
	MC	%	Moisture content
Heat	ΔQ	kJ/h	Heat flow rate
	ΔQ <sub>gen</sub>	kJ/h	Metabolic heat generation rate
	Q	kJ/kg	Heat of combustion for degraded organics
	h <sub>dry</sub>	kJ/kg	Enthalpy of dry air
	h <sub>vapor</sub>	kJ/kg	Enthalpy of water vapor

Subscript	Definition
in	Inlet
out	Outlet
s	Waste
nom	Nominal

act	Actual
air	Removed by airflow

## Acknowledgement

This work was supported by the 2017 Research Fund of the University of Seoul

## References

1. Brennan RB, Healy MG, Morrison L, et al (2016) Management of landfill leachate: The legacy of European Union Directives. *Waste Manag* 55:355–363. <https://doi.org/10.1016/j.wasman.2015.10.010>
2. European commission (1999) Council Directive 1999/31/EC on the landfill. *Off J Eur Communities* L182/14-23. <https://doi.org/10.1039/ap9842100196>
3. Juniper Consultancy Services Ltd (2005) *Mechanical-Biological Treatment: A Guide for Decision Makers, Processes, Policies and Markets*
4. Kanning K, Ketelsen K (2013) MBT – Best technology for treatment of moist MSW AD and / or biodrying prior to energy recovery. pp 328–342
5. Velis CA, Longhurst PJ, Drew GH, et al (2009) Biodrying for mechanical-biological treatment of wastes: A review of process science and engineering. *Bioresour Technol* 100:2747–2761. <https://doi.org/10.1016/j.biortech.2008.12.026>
6. Huiliñir C, Villegas M (2015) Simultaneous effect of initial moisture content and airflow rate on biodrying of sewage sludge. *Water Res* 82:118–28. <https://doi.org/10.1016/j.watres.2015.04.046>
7. Colomer-Mendoza FJ, Herrera-Prats L, Robles-Martínez F, et al (2013) Effect of airflow on biodrying of gardening wastes in reactors. *J Environ Sci (China)* 25:865–872. [https://doi.org/10.1016/S1001-0742\(12\)60123-5](https://doi.org/10.1016/S1001-0742(12)60123-5)
8. Adani F, Baido D, Calcaterra E, Genevini P (2002) The influence of biomass

- temperature on biostabilization-biodrying of municipal solid waste. *Bioresour Technol* 83:173–179. [https://doi.org/10.1016/S0960-8524\(01\)00231-0](https://doi.org/10.1016/S0960-8524(01)00231-0)
9. Navaee-Ardeh S, Bertrand F, Stuart PR (2010) Key variables analysis of a novel continuous biodrying process for drying mixed sludge. *Bioresour Technol* 101:3379–3387. <https://doi.org/10.1016/j.biortech.2009.12.037>
  10. Yang B, Zhang L, Lee Y, Jahng D (2013) Novel bioevaporation process for the zero-discharge treatment of highly concentrated organic wastewater. *Water Res* 47:5678–5689. <https://doi.org/10.1016/j.watres.2013.06.044>
  11. Yang B, Zhang L, Jahng D (2014) Importance of Initial Moisture Content and Bulking Agent for Biodrying Sewage Sludge. *Dry Technol* 32:135–144. <https://doi.org/10.1080/07373937.2013.795586>
  12. Zhao L, Gu WM, He PJ, Shao LM (2011) Biodegradation potential of bulking agents used in sludge bio-drying and their contribution to bio-generated heat. *Water Res* 45:2322–2330. <https://doi.org/10.1016/j.watres.2011.01.014>
  13. Song X, Ma J, Gao J, et al (2017) Optimization of bio-drying of kitchen waste: inoculation, initial moisture content and bulking agents. *J Mater Cycles Waste Manag* 19:496–504. <https://doi.org/10.1007/s10163-015-0450-3>
  14. Cai L, Gao D, Chen T Bin, et al (2012) Moisture variation associated with water input and evaporation during sewage sludge bio-drying. *Bioresour Technol* 117:13–19. <https://doi.org/10.1016/j.biortech.2012.03.092>
  15. Zhao L, Gu WM, He PJ, Shao LM (2010) Effect of air-flow rate and turning frequency on bio-drying of dewatered sludge. *Water Res* 44:6144–6152. <https://doi.org/10.1016/j.watres.2010.07.002>
  16. Nakasaki K, Nag K, Karita S (2005) Microbial succession associated with organic matter decomposition during thermophilic composting of organic waste. *Waste Manag Res* 23:48–56. <https://doi.org/10.1177/0734242X05049771>
  17. Chang JI, Tsai JJ, Wu KH (2005) Mathematical model for carbon dioxide evolution from the thermophilic composting of synthetic food wastes made of dog food. *Waste*

Manag 25:1037–1045. <https://doi.org/10.1016/j.wasman.2005.01.018>

18. Ahn HK, Richard TL, Choi HL (2007) Mass and thermal balance during composting of a poultry manure-Wood shavings mixture at different aeration rates. *Process Biochem* 42:215–223. <https://doi.org/10.1016/j.procbio.2006.08.005>
19. Spoehr HA, Milner H (1949) The chemical composition of *Chorella*; effect of environmental conditions. *Plant Physiol* 120–149. <https://doi.org/10.1104/pp.24.1.120>

**Figure captions:**

**Fig. 1** Schematic view of the reactor used in the bio-drying experiment

**Fig. 2** Experimental data and model output of run “50-3” (a) Temperature and CO<sub>2</sub> concentration profiles (Measured), (b) Rate of water mass changes in balance (Estimated), (c) Heat profiles (Estimated)

**Fig. 3** Comparison of actual removed water mass ( $W_{act}$ ) between experiment and model during entire experimental period

**Fig. 4** Temperature dependence of  $p_{vs}$  and  $X_{sat}$  and increase of water vapor pressure ( $p_v$ ) in bio-drying process

**Fig. 5** Relations between water removal rate and RH of inlet air under different AFR during w/o BIO period

**Fig. 6** CO<sub>2</sub> generation rate and moisture content profiles during entire experimental period (a) AFR 1 L/min, (b) AFR 3 L/min

**Fig. 7** Conceptual diagram of water removal rate in the bio-drying process

**Fig. 8** Water removal rate defined in Fig. 7 at the peak point of CO<sub>2</sub> concentration (a) AFR 1 L/min, (b) AFR 3 L/min

**Fig. 9** Removed water mass during w/ BIO period (a) Comparison of nominal removed water mass ( $W_{nom}$ ) and actual removed water mass ( $W_{act}$ ), (b) Effect of temperature increase ( $W_{nom}-W_{air}$ ,  $W_{nom}-W_{air}-W_{gen}$ ) on water removal compared with the effect of airflow ( $W_{air}$ )

**Fig. 10** Overall water removal mechanism in the bio-drying process

**Table 1.** Different variables and initial conditions in the experiments

Experimental condition							
Runs	Initial			Time days	Initial	Final	
	OC %	V L/min	RH $\pm$ SD %		M <sub>O</sub> kg	M <sub>O</sub> kg	W kg
10-1	10	1	61.1 $\pm$ 4.7	19	0.314	0.000	1.842
25-1	25	1	23.8 $\pm$ 5.0	16	0.786	0.375	1.404
50-1	50	1	23.8 $\pm$ 5.5	16	1.571	0.879	1.420
75-1	75	1	15.0 $\pm$ 7.2	32	2.357	1.475	0.919
100-1	100	1	33.9 $\pm$ 6.1	26	3.143	2.181	1.070
10-2	10	2	59.4 $\pm$ 3.2	12	0.314	0.053	1.603
25-2	25	2	15.4 $\pm$ 5.3	10	0.786	0.484	1.090
50-2	50	2	23.3 $\pm$ 5.1	14	1.571	1.094	0.817
75-2	75	2	10.1 $\pm$ 1.7	14	2.357	1.815	0.719
100-2	100	2	36.3 $\pm$ 6.8	16	3.143	2.639	0.629
10-3	10	3	59.4 $\pm$ 3.2	11	0.314	0.062	1.303
25-3	25	3	16.9 $\pm$ 5.4	7	0.786	0.612	0.996
50-3	50	3	14.0 $\pm$ 4.7	8	1.571	1.318	0.884
75-3	75	3	9.9 $\pm$ 1.9	10	2.357	2.003	0.579
100-3	100	3	33.6 $\pm$ 6.7	13	3.143	2.644	0.350



**Table 2.** Equations used for mass and heat balance

Contents	Equation
Airflow rate of outlet air (m <sup>3</sup> /h)	$V_{out} = \frac{(273.15 + T_{out})}{(273.15 + T_{in})} \times V_{in} \quad (3)$
Water vapor per unit air volume (g/m <sup>3</sup> )	$X = \frac{217 \times pv}{273.15 + T} \quad (4)$
Water vapor pressure (Pa)	$pv = RH \times pvs \quad (5)$
Saturated water vapor pressure (Pa)	$pvs = 6.1078 \times 10^{\frac{7.5 \times T}{T + 237.3}} \quad (6)$
Organic degradation	$C_{21}H_{36}O_{14}N + 22.3 O_2 \rightarrow 21 CO_2 + 16.3 H_2O + NH_3 + Heat \quad (7)$
Generated CO <sub>2</sub> (kmol/h)	$\Delta C_{gen} = [(V \times CO_2)_{out} - (V \times CO_2)_{in}] \times \frac{1}{100} \times \frac{1 \text{ kmol } CO_2}{22.4 \text{ m}^3} \quad (8)$
Degraded organics (kg/h)	$\Delta M_O = \frac{1}{21} \times \Delta C_{gen} \times \frac{533.2 \text{ kg}}{1 \text{ kmol}} \quad (9)$
Metabolic water (kg/h)	$\Delta w_{gen} = \frac{16.3}{21} \times \Delta C_{gen} \times \frac{18 \text{ kg}}{1 \text{ kmol}} \quad (10)$
Heat generation (kJ/h)	$\Delta Q_{gen} = \Delta M_O \times 20406 \text{ kJ/kg} \quad (11)$
Heat transfer in air flow (kJ/h)	$\Delta Q = h_{dry} \times \rho_a \times V + h_{vapor} \times X \times 10^{-3} \times V \quad (13)$
Enthalpy of dry air (kJ/kg)	$h_{dry} = 1.006 \times T \quad (14)$
Enthalpy of water vapor (kJ/kg)	$h_{vapor} = 1.805 \times T + 2501 \quad (15)$
Density of dry air (kg/m <sup>3</sup> )	$\rho_a = 1.293 \times \frac{273.15}{273.15 + T} \quad (16)$

**Fig. 1** Schematic view of the reactor used in the bio-drying experiment

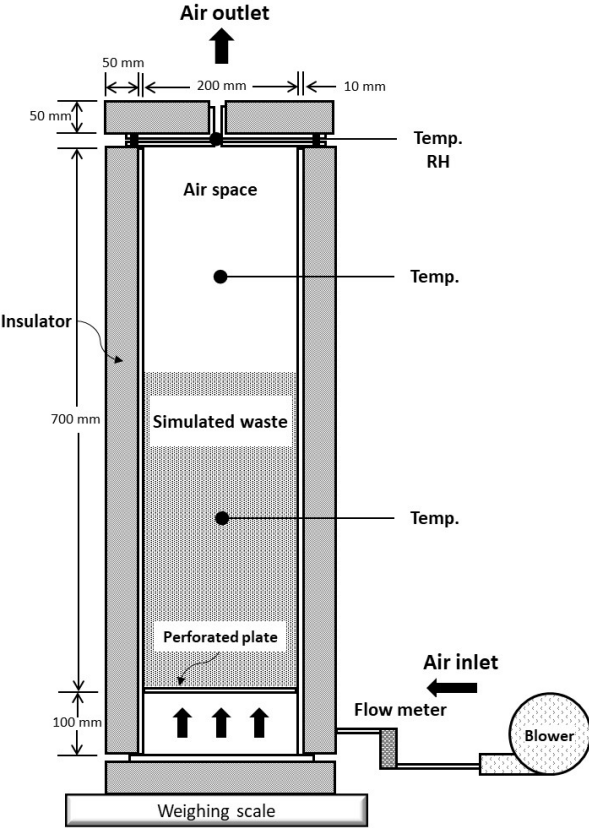


**Fig.2** Experimental data and model output of run “50-3” (a) Temperature and CO<sub>2</sub> concentration profiles (Measured), (b) Rate of water mass changes in balance (Estimated), (c) Heat profiles (Estimated)

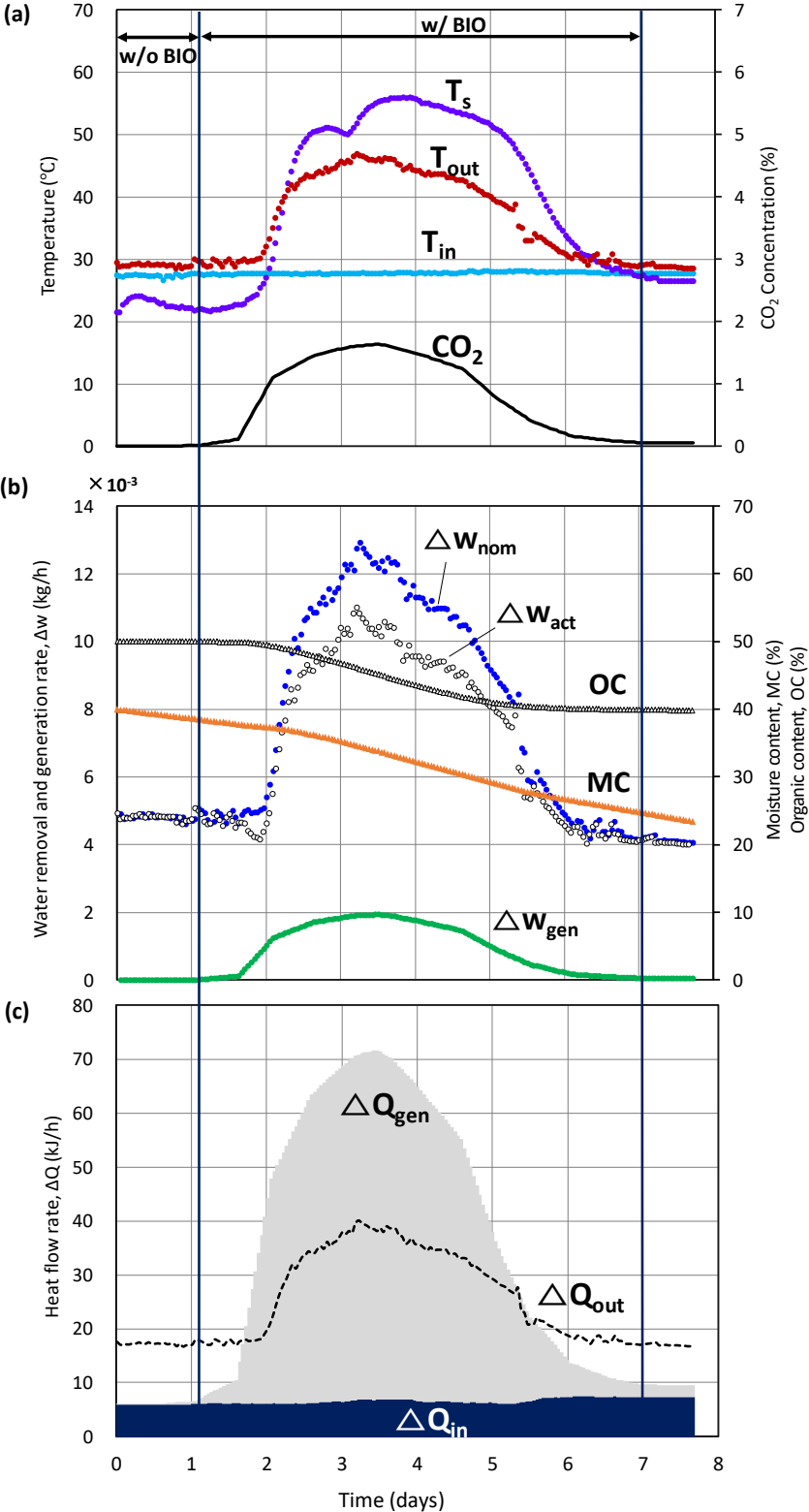


**Fig. 3** Comparison of actual removed water mass ( $W_{act}$ ) between experiment and model during entire experimental period

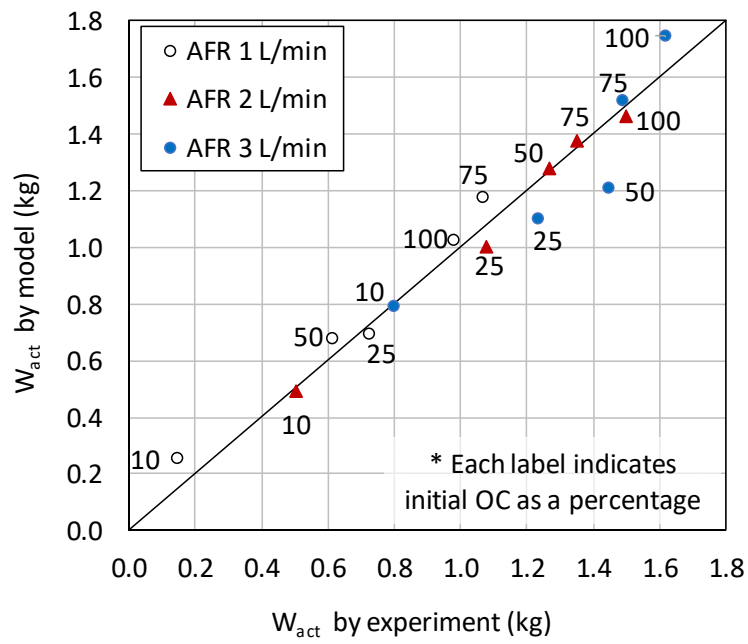


**Fig. 4** Temperature dependence of  $p_{vs}$  and  $X_{sat}$  and increase of water vapor pressure ( $p_v$ ) in bio-drying process

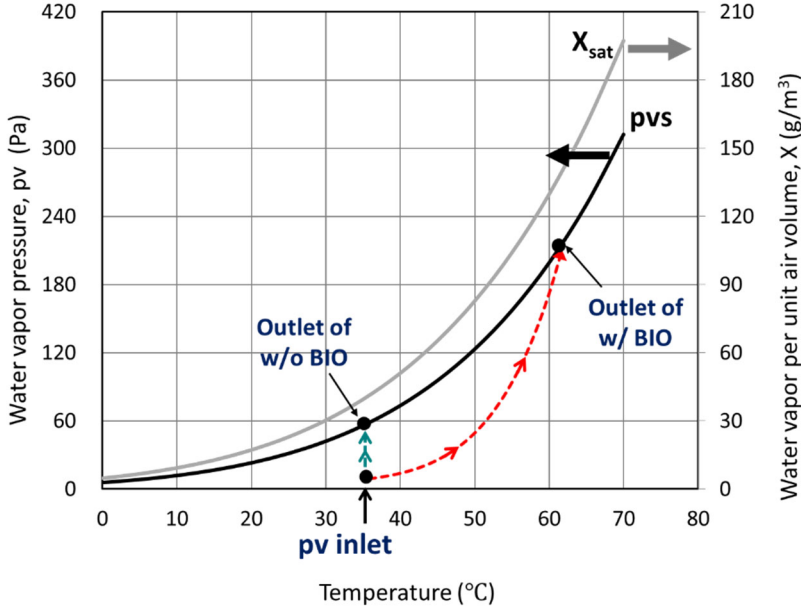


**Fig. 5** Relations between water removal rate and RH of inlet air under different AFR during w/o BIO period

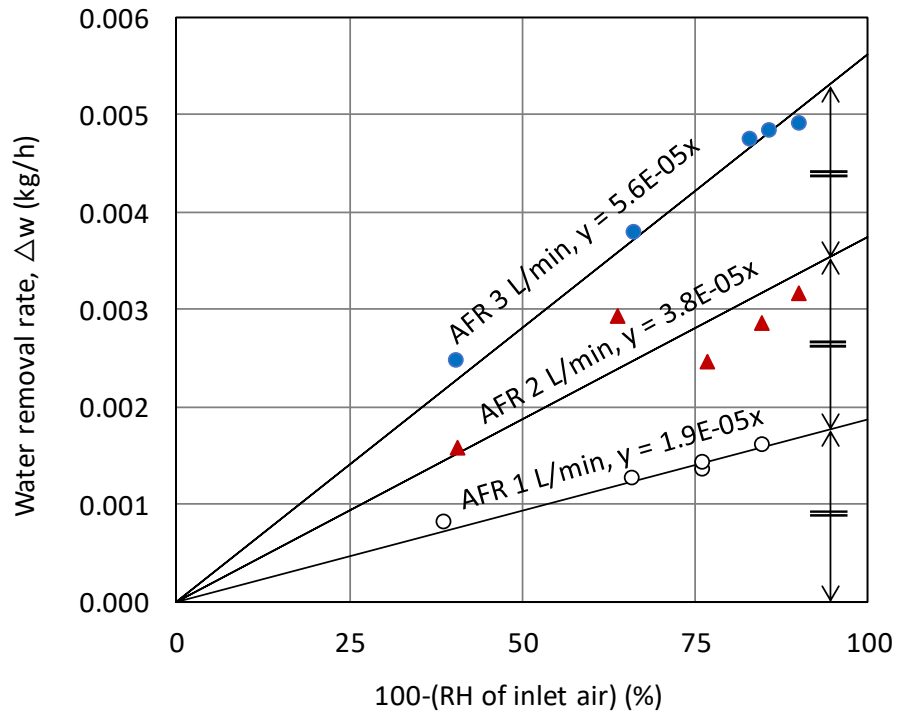


**Fig. 6** CO<sub>2</sub> generation rate and moisture content profiles during entire experimental period (a) AFR 1 L/min, (b) AFR 3 L/min

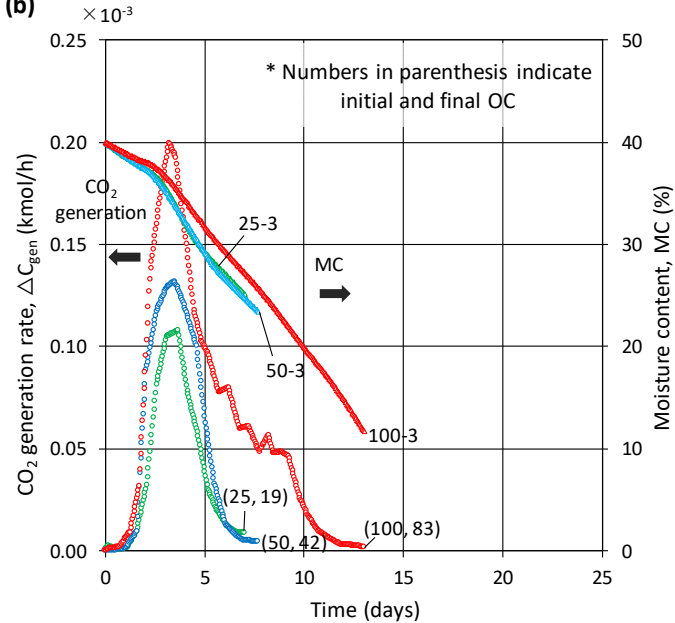
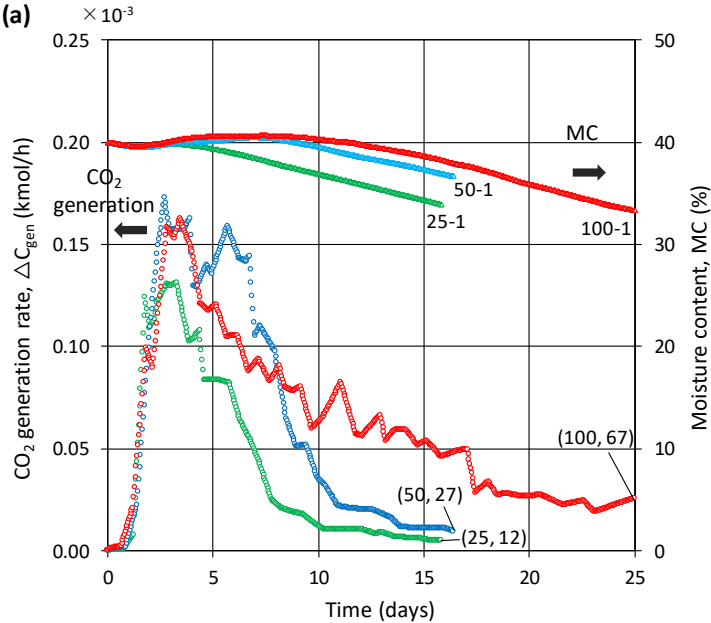


**Fig. 7** Conceptual diagram of water removal rate in the bio-drying process

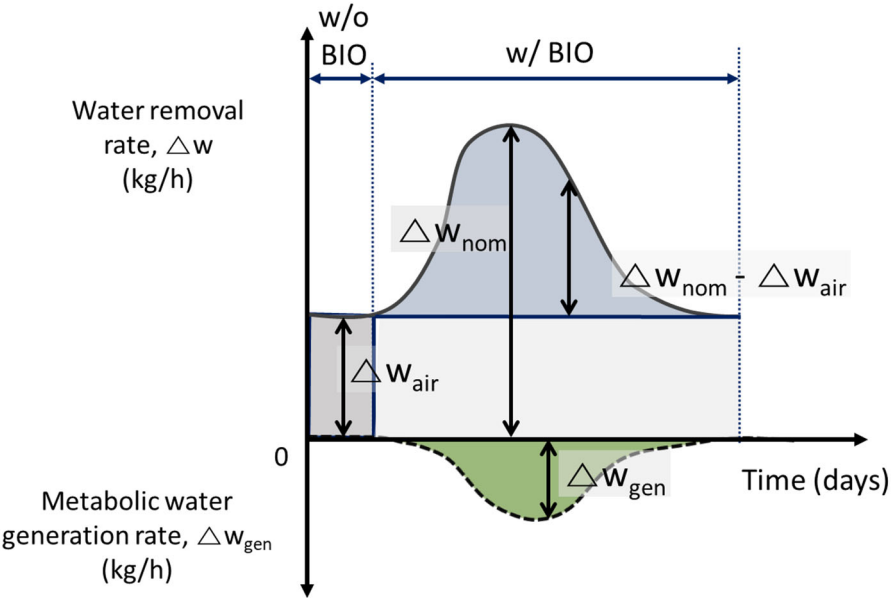




**Fig. 8** Water removal rate defined in Fig. 7 at the peak point of CO<sub>2</sub> concentration (a) AFR 1 L/min, (b) AFR 3 L/min

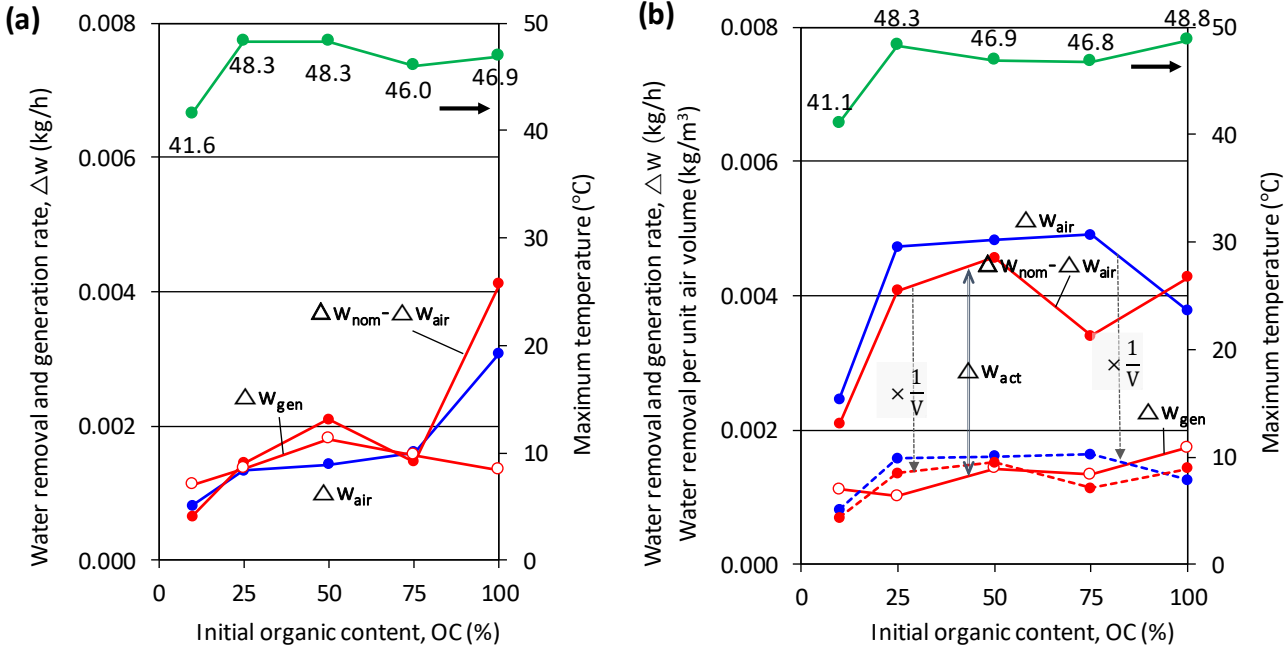


**Fig. 9** Removed water mass during w/ BIO period (a) Comparison of nominal removed water mass ( $W_{nom}$ ) and actual removed water mass ( $W_{act}$ ), (b) Effect of temperature increase ( $W_{nom}-W_{air}$ ,  $W_{nom}-W_{air}-W_{gen}$ ) on water removal compared with the effect of airflow ( $W_{air}$ )

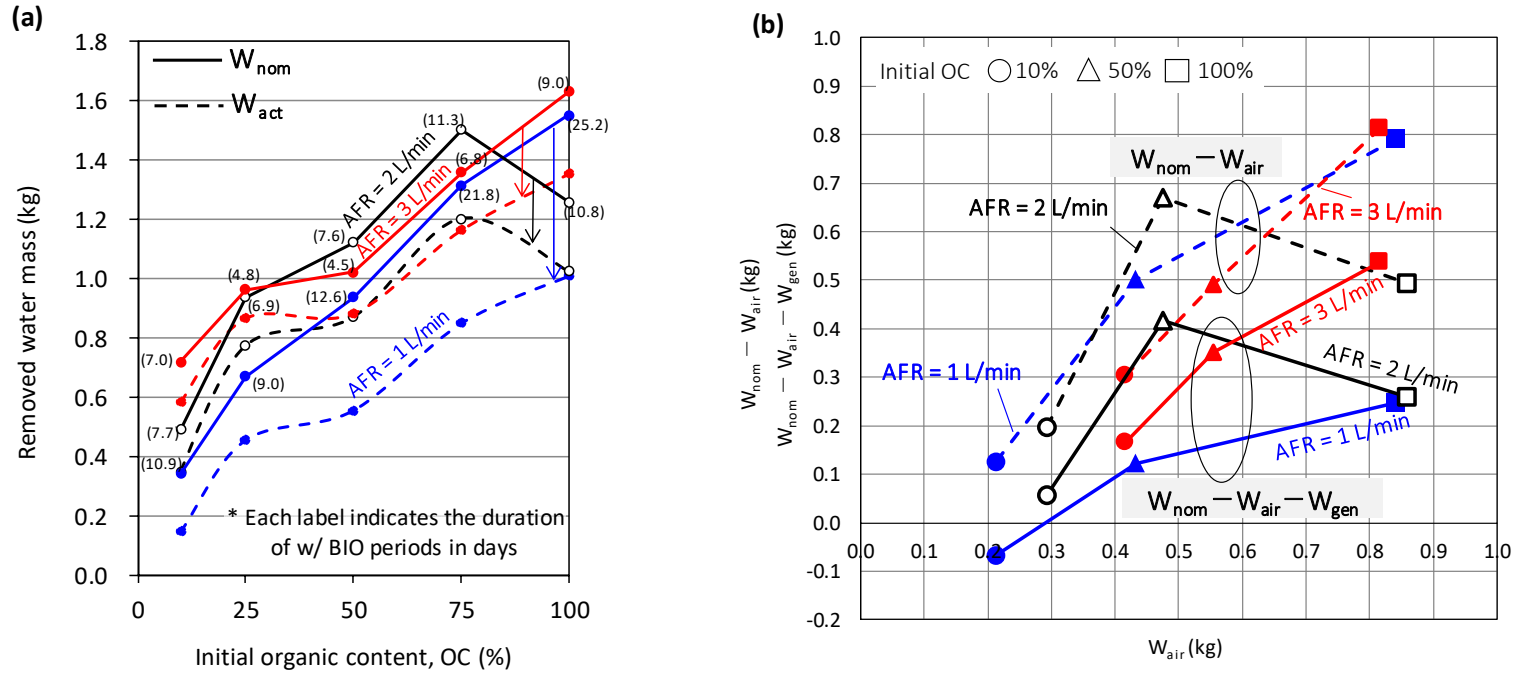


**Fig. 10** Overall water removal mechanism in the bio-drying process

